Special Issue on Chemistry

Aloe vera Plant Extract - Assisted Green Synthesis of SnO_2 Nanoparticles with Environmental Catalytic Activity

C. Rama and T. Lakshmikandhan

Issue Editor
Dr. A. Manikandan

Research Journal of Agricultural Sciences
An International Journal

P- ISSN: 0976-1675
E- ISSN: 2249-4538

Volume: 13
Issue: Special

Res. Jr. of Agril. Sci. (2022) 13(S): 006–011

CARAS

Res. Jr. of Agril. Sci. (2022)
13(Special): 006–011

www.rjas.org

ISSN: 0976-1675 (P)
ISSN: 2249-4538 (E)

Full Length Research Article

Aloe vera Plant Extract - Assisted Green Synthesis of SnO_2 Nanoparticles with Environmental Catalytic Activity

C. Rama[1] and T. Lakshmikandhan*[2]

Received: 16 Nov 2021 | Revised accepted: 30 Jan 2022 | Published online: 25 Feb 2022

ABSTRACT

SnO_2 nanoparticles were produced in aqueous solution utilizing green method without the need of any templates, catalysts, or organic reagents in this study. Powder X-ray diffraction (XRD), scanning electron microscopy (SEM), and transmission electron microscopy (TEM), high-resolution TEM (HRTEM), Fourier transform infrared (FT-IR) spectroscopy measurements were used to characterize the as-prepared SnO_2 nanoparticles. Microwave irradiation can create SnO_2 with a consistent size and shape, as well as a high crystallinity. A probable production mechanism of SnO_2 nanoparticles was hypothesized based on experimental results. Furthermore, environmental catalytic performance of the obtained SnO_2 nanoparticles in the degradation of Rhodamine B (RhB) in aqueous solution was discovered, showing that these SnO_2 nanoparticles are very promising for wastewater treatment.

Key words: SnO_2 nanoparticles, Green method, X-ray diffraction, Microwave irradiation, Rhodamine B

Chemists are being challenged to investigate environmentally friendly techniques to synthesis target materials as cleaner and more benign chemical processes based on green chemistry principles are developed [1]. Synthetic chemists identified "safer solvents" and "better energy efficiency" as two of the 12 principles of green chemistry [1–4]. Recently, there has been a lot of effort put towards developing and using unconventional solvents for material synthesis. Recently, there has been a lot of effort put towards developing and using unconventional solvents for material synthesis [5, 6]. Water, supercritical carbon dioxide, ionic liquids, perfluorinated solvents, and other unusual media are examples. Water is the most readily available and environmentally friendly of these unusual solvents. Meanwhile, microwave heating has been proven and approved as a promising technology for rapid volumetric heating, high-response rate and selectivity, short reaction time, and high yield when compared to conventional heating methods [7–12]. This allowed for the rapid processing of materials in a short amount of time while maintaining great energy efficiency [13]. Microwaves are now often employed in a wide range of chemistry applications, from analytical chemistry to liquid-phase organic synthesis to solid-state processes.

Because of their unique physical and chemical properties, SnO_2 in various phases has drawn a lot of research and has a lot of potential as selective heterogeneous catalysts, adsorbents, and battery materials [14–21]. They've been employed in a variety of industrial catalytic processes, including ozone decomposition, photocatalytic oxidation of organic pollutants, nitric oxide reduction, selective carbon monoxide oxidation, hydrogen peroxide breakdown, and so on [22-26]. Nanostructured materials have been increasingly appealing in recent years due to their favourable and increased physical and chemical properties. The fabrication of SnO_2 nanostructures with various morphologies has received a lot of attention [27-30]. However, only a few studies have been published on the synthesis of SnO_2 nanoparticles using microwave irradiation [31-35].

We present a green approach for synthesizing SnO_2 nanoparticles with uniform size and well-defined shape in aqueous solution using a microwave-assisted process [36-40]. This method has at least two clear benefits: the process is quick and easy, and no high-pressure or high-temperature equipment is required [41-45]. Furthermore, we discovered that as-prepared SnO_2 nanoparticles performed admirably on the Fenton oxidation of Rhodamine B (RhB) in aqueous solution, indicating that SnO_2 nanoparticles are potential materials for environmental catalysis.

MATERIALS AND METHODS

Chemicals

All of the chemicals used in this investigation were bought from Sinopharm Chemical Reagent Co. Ltd. and were of analytical quality (Shanghai China). In all of the trials, deionized water was used.

Preparation of the SnO_2 samples

* **T. Lakshmikandhan**
kandh84@gmail.com

1-2 Department of Chemistry, Bharath Institute of Higher Education and Research (BIHER), Chennai - 600 073, Tamil Nadu, India

Microwave irradiation was used to make SnO_2 nanoparticles in an aqueous solution Aloe vera extract and $Sn(NO_3)_2$ were dissolved in 20 mL distilled water in a 100 mL silica crucible in an usual technique. The resultant aqueous solution was then reacted for 10 minutes using microwave irradiation generated by a microwave oven. The resulting solid product was rinsed with deionized water to eliminate any ions that may have remained in the final goods, and then dried in an air oven at 70°C.

Characterization

On a Bruker D8 Advance X-ray diffractometer, powder diffraction patterns were acquired using Cu Kα radiation (λ= 1.54178Å). A LEO 1450VP scanning electron microscope was used to create the images. On a Philips CM-120 electron microscope, a transmission electron microscopy (TEM) investigation was performed. The TEM samples were made by dispersing the final powders in ethanol and then dropping the dispersion onto carbon–copper grids. A high-resolution transmission electron microscope (HRTEM; JEOL JSM-2010 microscope) operating at 200 kV was used to examine the powders placed on a copper grid. The usual KBr pellet approach was used to record Fourier transforms infrared (FT-IR) spectra were on a Nicolet Nexus spectrometer.

Environmental catalytic activity of the as-prepared SnO_2 nanoparticles

The catalytic reaction was carried out in a 250mL glass flask with 100mL of RhB dye solution ($5mgL^{-1}$) and 100mg of produced SnO_2 nanostructure catalysts without any pH adjustments. The final solution had a pH of approximately 6.2, which was neutral. The mixture was allowed to react at room temperature under continuous stirring after adding 2mL of 30 wt. percent H_2O_2 solution. The solution was immediately centrifuged to remove the catalyst particles, which tend to scatter the incident beam, before UV–vis absorption measurements. Colorimetry with a U-3310 UV–vis spectrometer (HITACHI) was used to measure the content of RhB at its maximum absorption wavelength of 555nm at 10-minute intervals.

RESULTS AND DISCUSSION

XRD analysis

The phase structure of the as-prepared SnO_2 samples was studied using X-ray diffraction. The X-ray diffraction (XRD) pattern of the SnO_2 product produced in aqueous solution under microwave irradiation is shown in (Fig 1). The pattern of the as-prepared sample closely resembles the standard patterns of SnO_2 (JCPDS file no. 14-644), where the diffraction peaks can be attributed to the reflection of the SnO_2 planes [46-50]. There are no peaks for other contaminants, indicating that the as-synthesized product is quite pure. Furthermore, the broadening of the XRD peaks reveals the material's nanocrystalline structure. According to the XRD pattern, crystalline SnO_2 samples can be easily generated using this environmentally friendly process.

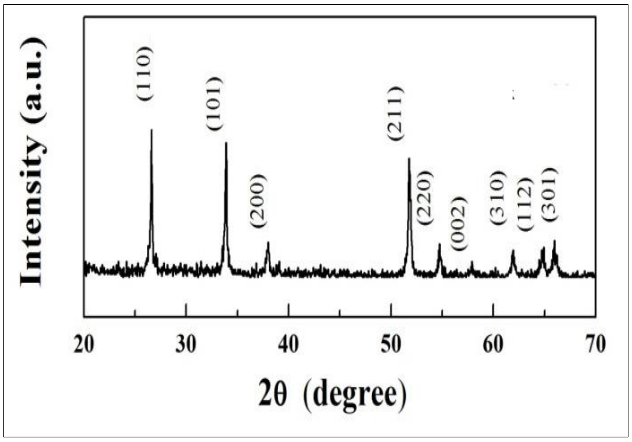

Fig 1 XRD pattern of SnO_2 nanoparticle

SEM analysis

Scanning electron microscopy was used to examine the morphology of the obtained sample. Scanning electron microscopy (SEM) pictures of the product created under microwave irradiation are shown in (Fig 2). We discovered that the SnO_2 nanoparticles included a large number of particles with a ratio of nearly 100 percent (Fig 2). The nanoplates are clearly defined and homogeneous. The nanoparticles are 15–20nm in diameter, according to a high-magnification SEM photograph (Fig 2).

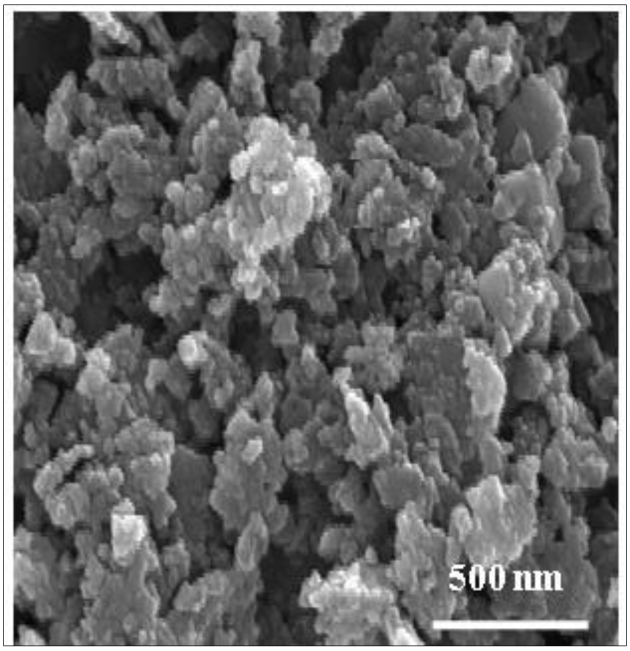

Fig 2 SEM images of SnO_2 nanoparticles

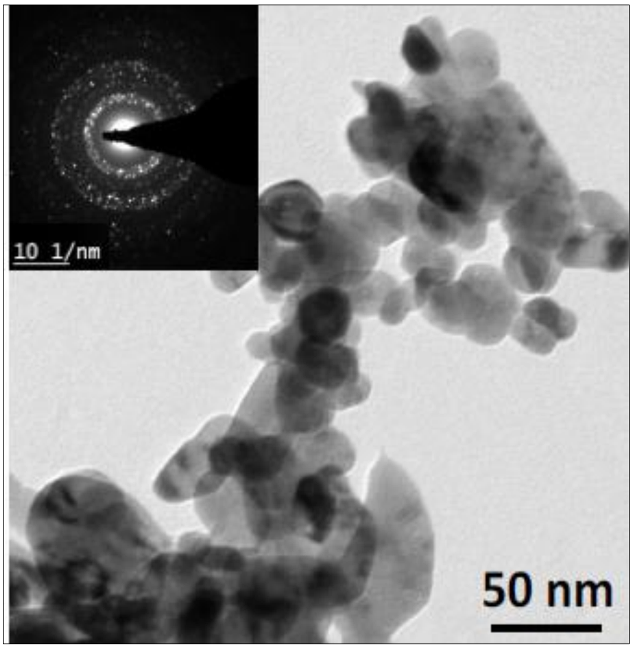

Fig 3 TEM images of SnO_2 nanoparticles

TEM analysis

The crystal structure of the produced nanoparticles was further investigated using transition electron microscopy (TEM) and high-resolution transition electron microscopy (HRTEM) (Fig 3). The plate-like structure of the as-prepared sample is confirmed by TEM imaging (Fig 3) nanoparticles diameters range from 15 to 20 nm. HRTEM revealed the single-crystal nature of the nanoparticles. The distance between adjacent lattice planes of SnO_2 nanoparticles is roughly 2.42Å, which corresponds to the distance between [51] crystal planes of manganese oxide's gamma phase (JCPDS file no. 14-644).

FT-IR analysis

The functional groups on the surface of the final sample were identified using the FT-IR spectra. The spectra of SnO_2 nanoparticles generated under microwave irradiation is shown in (Fig 4). The stretching vibrations of hydrogen-bonded surface water molecules and hydroxyl groups are thought to be connected with the broad band at 3395cm^{-1}. Furthermore, the bands at 1614 and 1384cm^{-1} correlate to the presence of a substantial number of residual hydroxyl groups, implying that residues of adsorbed water are vibrating in the O−H mode. The Sn−O vibrations of SnO_2 nanoparticles are responsible for the band at 525cm^{-1}. The results of the FTIR analysis provided here are congruent with those found in the literature [51–56]. Based on IR spectra, no organic groups were observed to be adsorbed on the surface.

Preliminary environmental catalytic activity

One of the most successful advanced oxidation processes (AOPs) for wastewater treatment is the Fenton-like reaction. However, when employing the classic Fenton process to treat wastewater, pH is a significant operating parameter because these Fenton systems can only work efficiently in very acidic conditions (pH 2–3). To achieve this pH requirement, powerful acids must usually be added to wastewater before typical Fenton reactions may be used. This prevents the classic Fenton procedure from being used in wastewater treatment in the future. As a result, numerous researchers began to create active heterogeneous systems to allow the Fenton reaction to operate at pH levels close to neutral [57–60].

For H_2O_2 breakdown, SnO_2 nanoparticles can act as Fenton-like catalysts. We studied the catalytic efficacy of SnO_2 nanoparticles produced by microwave irradiation on the Fenton oxidation of RhB dye in this study (Fig 5). We discovered that using SnO_2 nanoparticles as the catalyst, a Fenton-like system could efficiently decompose RhB in aqueous solution. In the presence of both SnO_2 nanoparticles and H_2O_2, however, considerable deterioration occurred [61-65]. Surprisingly, in the presence of SnO_2 nanoparticles, RhB degradation might reach 65% in 5 minutes at neutral pH. As a result, the as-prepared SnO_2 nanoparticles have a high-Fenton oxidation activity on RhB degradation, making them ideal for environmental remediation. Environmental catalytic uses of SnO_2 nanoparticles are being studied in more depth.

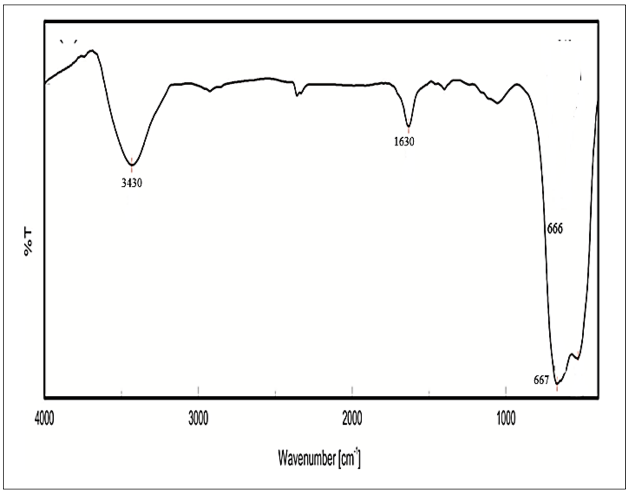

Fig 4 FT-IR analysis of SnO_2 samples

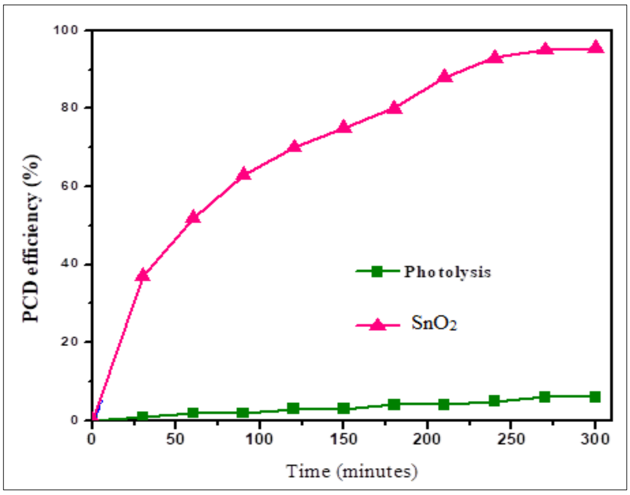

Fig 5 PCD efficiency of SnO_2 samples

CONCLUSION

Using microwave irradiation, we established a green technique for synthesizing SnO_2 nanoparticles in aqueous solution. The synthesis route does not require templates, catalysts, or organic reagents. In addition, the SnO_2 nanoparticles excelled at catalytic discolouration of RhB via Fenton reactions. For the manufacture of environment catalysts, this green synthetic technique and the capability of scale manufacturing of SnO_2 nanoparticles are particularly appealing.

LITERATURE CITED

1. Renuga R, A. Manikandan, J. A. Mary, A. Muthukrishnaraj, A. Khan, S. Srinivasan, B. Abdullah M. Al Alwan, Khedher KM. 2021. Enhanced Magneto-Optical, Morphological, and Photocatalytic Properties of Nickel-Substituted SnO_2 Nanoparticles. *Jr. Supercond. Nov. Magn*. 34: 825-836.
2. Vinosha PA, A. Manikandan, R. Ragu, A. Dinesh, P. Paulraj, Y. Slimani, M.A. Almessiere, A. Baykal, J. Madhavan, B. Xavier, Nirmala GF. 2021. Exploring the influence of varying pH on structural, electro-optical, magnetic and photo-Fenton properties of mesoporous $ZnFe_2O_4$ nanocrystals. *Environmental Pollution* 272: 115983
3. Ajeesha TL, A. Ashwini, M. George, A. Manikandan, J. A. Mary, Y. Slimani, M. A. Almessiere, Baykal A. 2021. Nickel substituted $MgFe_2O_4$ nanoparticles via co-precipitation method for photocatalytic applications. *Physica B: Condensed Matter* 606: 412660.
4. Senthil RA, S. Osman, J. Pan, A. Khan, V. Yang, T. R. Kumar, Y. Sun, Manikandan A. 2020. One-pot preparation of AgBr/α-Ag_2WO_4 composites with superior photocatalytic activity under visible-light irradiation. *Colloid. Surf. A: Physicochem. Eng. Aspect*. 586: 124079.

5. Muthukrishnaraj A, SS Kalaivani, A Manikandan, H. P. Kavitha, R Srinivasan, Balasubramanian N. 2020. Sonochemical synthesis and visible light induced photocatalytic property of reduced graphene oxide@ ZnO hexagonal hollow rod nanocomposite. *Journal of Alloys and Compounds* 83625: 155377.
6. Rathinavel S, R. Deepika, D. Panda, Manikandan A. 2021. Synthesis and characterization of $MgFe_2O_4$ and $MgFe_2O_4$/rGO nanocomposites for the photocatalytic degradation of methylene blue. *Inorganic and Nano-Metal Chemistry* 51(2): 210-217.
7. Senthil RA, S. Osman, J. Pan, Y. Sun, T. R. Kumar, Manikandan A. 2019. A facile hydrothermal synthesis of visible-light responsive $BiFeWO_6/MoS_2$ composite as superior photocatalyst for degradation of organic pollutants *Ceram. Int*. 45: 18683-18690.
8. George M, T.L. Ajeesha, A. Manikandan, A. Anantharaman, R.S. Jansi, E. R. Kumar, Y. Slimani, M.A. Almessiere, Baykal A. 2021. Evaluation of Cu-$MgFe_2O_4$ spinel nanoparticles for photocatalytic and antimicrobial activates. *Jr. Phys. Chem. Solids* 153:110010.
9. Elayakumar K, A. Manikandan, A. Dinesh, K. Thanrasu, K. K. Raja, R. Thilak Kumar, Y. Slimani, S. K. Jaganathan, Baykal A. 2019. Enhanced magnetic property and antibacterial biomedical activity of Ce^{3+} doped $CuFe_2O_4$ spinel nanoparticles synthesized by sol-gel method. *Jr. Magn. Magn. Mater*. 478: 140-147.
10. Babitha N, L. S. Priya, S. R. Christy, A. Manikandan, A. Dinesh, M. Durka, Arunadevi S. 2019. Enhanced Antibacterial Activity and Photo-Catalytic Properties of ZnO Nanoparticles: Pedalium Murex Plant Extract-Assisted Synthesis. *Jr. Nanosci. Nanotech*. 19: 2888–2894.
11. Al-Jameel SS, S. Rehman, M. A. Almessiere, F. A. Khan, Y. Slimani, N. S. Al-Saleh, A. Manikandan, E. A. Al-Suhaimi, Baykal A. 2021. Anti-microbial and anti-cancer activities of $MnZnDy_xFe_{2-x}O_4$ ($x \leq 0.1$) nanoparticles. *Artificial Cells, Nanomed. Biotech*. 49: 493-499.
12. Elayakumar K, A. Dinesh, A. Manikandan, P. Murugesan, G. Kavitha, S. Prakash, R. T. Kumar, S. K. Jaganathan, Baykal A. 2019. Structural, morphological, enhanced magnetic properties and antibacterial bio-medical activity of rare earth element (REE) Cerium (Ce^{3+}) doped $CoFe_2O_4$ nanoparticles. *Jr. Magn. Magn. Mater*. 476: 157-165.
13. Manikandan A, M. Durka, Antony SA 2015. Role of Mn^{2+} doping on structural, morphological and opto-magnetic properties of spinel $Mn_xCo_{1-x}Fe_2O_4$ (x = 0.0, 0.1, 0.2, 0.3, 0.4 and 0.5) nano-catalysts. *Journal of Superconductivity and Novel Magnetism* 28: 2047-2058.
14. Manikandan A, E. Hema, M. Durka, K. Seevakan, T. Alagesan, Antony SA. 2015. Room temperature ferromagnetism of magnetically recyclable photocatalyst of $Cu_{1-x}Mn_xFe_2O_4$-TiO_2 ($0.0 \leq x \leq 0.5$) nano-composites. *Journal of Superconductivity and Novel Magnetism* 28: 1783-1795.
15. Manikandan A, M. Durka, K. Seevakan, Antony SA. 2015. A novel one-pot combustion synthesis and opto-magnetic properties of magnetically separable spinel $Mn_xMg_{1-x}Fe_2O_4$ ($0.0 \leq x \leq 0.5$) nano-photocatalysts. *Journal of Superconductivity and Novel Magnetism* 28: 1405-1416.
16. Murugan E, Vimala G. 2011. Effective functionalization of multiwalled carbon nanotube with amphiphilic poly(propyleneimine) dendrimer carrying silver nanoparticles for better dispersability and antimicrobial activity. *Journal of Colloid and Interface Science* 357(2): 354-365.
17. Pubby K, Narang SB. 2019. Influence of grain size and porosity on X-band properties of Mn-Zr substituted Ni-Co ferrites. *Mater. Lett*. 244: 186-191.
18. Sonia MML, S. Anand, S. Blessi, S. Pauline, Manikandan A. 2018. Effect of surfactants (PVB/EDTA/CTAB) assisted sol-gel synthesis on structural, magnetic and dielectric properties of $NiFe_2O_4$ nanoparticles. *Ceramics International* 44: 22068-22079.
19. Murugan E, Rangasamy R. 2011. Development of stable pollution free TiO_2/Au nanoparticle immobilized green photo catalyst for degradation of methyl orange. *Journal of Biomedical Nanotechnology* 7(1): 225-228.
20. Praveena K, K. Sadhana, S. Bharadwaj, Murthy SR. 2010. Fabrication of dc–dc converter using nanocrystalline Mn–Zn ferrites. *Mater. Res. Innovations* 14: 102-106.
21. Huang R, D. Zhang, Tseng KJ. 2008. Determination of Dimension-Independent Magnetic and Dielectric Properties for Mn–Zn Ferrite Cores and Its EMI Applications. *IEEE Trans*. *Electromagn. Compat*. 50: 597-602.
22. Murugan E, S Santhoshkumar, S Govindaraju, Palanichamy M. 2021. Silver nanoparticles decorated g-C_3N_4: An efficient SERS substrate for monitoring catalytic reduction and selective Hg^{2+} ions detection. *Spectrochimica Acta Part A: Molecular and Biomolecular Spectroscopy* 246: 119036.
23. Xie T, H. Li, C. Liu, J. Yang, T. Xiao, Xu L. 2018. Magnetic photocatalyst BiVO4/Mn-Zn ferrite/reduced graphene oxide: Synthesis strategy and its highly photocatalytic activity. *Nanomaterials* 8: 380.
24. Shen CQ, H.N. Ji, J. Wu, N. Zhu, J.Q. Niu, H.D. Li, Niu XB. 2018. Synthesis and characterization of MnZn Ferrite Nanoparticles for Biomedical Applications. *In*: 2018 IEEE International Conference on Applied Superconductivity and Electromagnetic Devices (ASEMD), IEEE. pp 1-2.
25. Anwar A, S. Zulfiqar, M. A. Yousuf, S. A. Ragab, Muhammad Azhar Khand, Imran Shakir, Warsi MF. 2020. Impact of rare earth Dy^{+3} cations on the various parameters of nanocrystalline nickel spinel ferrite. *Jr. Mater. Res. Technology* 9: 5313-5325.
26. Shah J, R.K. Kotnala, B. Singh, Kishan H. 2007. Microstructure-dependent humidity sensitivity of porous $MgFe_2O_4$–CeO_2 ceramic. *Sens. Actuators B Chem*. 128: 306-311.
27. Khomskii DI. 2006. Multiferroics: Different ways to combine magnetism and ferroelectricity. *Journal of Magn. Magn. Mater*. 306: 1-8.
28. Yin L, Mi W. 2018. Progress in $BiFeO_3$-based heterostructures: materials, properties and applications. *Nanoscale* 12: 477.
29. Xueyao H, Xiaocha Wang, Wenbo M. 2018. Progress in Fe_3O_4-based multiferroic heterostructures. *Journal of Alloy Compd*., 765: 1127-1138.
30. Back M, E. Trave, R. Marin, N. Marzocco, D. Cristofori, Riello P. 2014. Energy Transfer in Bi- and Er-Codoped Y_2O_3 Nanocrystals: An Effective System for Rare Earth Fluorescence Enhancement. *Jr. Phys. Chem. A*., 118: 30071-30078.

31. Pal M, P. Brahrma, Chakravorty D. 1996. Magnetic and electrical properties of nickel-zinc ferrites doped with bismuth oxide. *Jr. Magn. Magn. Mater*. 152: 370-374.
32. Pal M, P. Brahrma, Chakravorty D. 1998. AC conductivity in bismuth oxide doped nickel-zinc ferrites. *Jr. Phys. Soc. Japan* 67: 2847-2851.
33. Angadi VJ, K. Manjunatha, S.P. Kubrin, A.T. Kozakov, A.G. Kochur, A.V. Nikolskii, I.D. Petrov, S.I. Shevtsova, Ayachit NH. 2020. Crystal structure, valence state of ions and magnetic properties of $HoFeO_3$ and $HoFe_{0.8}Sc_{0.2}O_3$ nanoparticles from X-ray diffraction, X-ray photoelectron, and Mössbauer spectroscopy data. *Jr. Alloy Compd*. 842: 155805.
34. Sathisha IC, K. Manjunatha, V. J. Angadi, Reddy RK. 2020. Structural, Microstructural, Electrical, and Magnetic Properties of $CuFe_{2-(x+y)}Eu_xSc_yO_4$ (where x and y vary from 0 to 0.03) Nanoparticles. *Jr. Supercond. Nov. Magn*. 33: 3963-3973.
35. Manjunatha K, V. J. Angadi, R. Rajaramakrishna, Pasha UM. 2020. Role of 5 mol% Mg-Ni on the structural and magnetic properties of cobalt chromates crystallites prepared by solution combustion technique. *Journal of Supercond. Nov. Magn*. 33: 2861-2866.
36. Ding F, J. Lin, T. Wu, Zhong H. 2020. Scanning electron microscopy (SEM), energy-dispersive X-ray (EDX) spectroscopy and nuclear radiation shielding properties of [α-Fe3+O(OH)]-doped lithium borate glasses. *Appl. Phys. A*, 126: 221.
37. Thakur P, Deepika Chahar, Shilpa Taneja, Nikhil Bhalla, Thakur A. 2020. A review on MnZn ferrites: Synthesis, characterization and applications. *Ceram. Int*. 46(10): 15740-15763.
38. Manjunatha K, K.M. Srininivasamurthy C.S. Naveen, Y.T. Ravikiran, E.I. Sitalo, S.P. Kubrin, S. Matteppanavar, N. S. Reddy, Angadi VJ. 2019. Observation of enhanced humidity sensing performance and structure, dielectric, optical and DC conductivity studies of scandium doped cobalt chromate. *Jr. Mater. Sci: Mater. Electron*. 30: 17202-17217.
39. Lakshmiprasanna HR, K. Manjunatha, V. J. Angadi, U. Mahaboob Pasha, Husain J. 2020. Effect of cerium on structural, microstructural, magnetic and humidity sensing properties of Mn–Bi ferrites. *Nano-Struct. Nano-Objects* 24: 100608.
40. Sunilkumar A, S. Manjunatha, T. Machappa, B. Chethan, Ravikiran YT. 2019. A tungsten disulphide–polypyrrole composite-based humidity sensor at room temperature. *Bull. Mater. Sci*. 42: 271.
41. Pratibha S, B. Chethan, Y.T. Ravikiran, N. Dhananjaya, Angadi VJ. 2020. Enhanced humidity sensing performance of Samarium doped Lanthanum Aluminate at room temperature. *Sensors Actuators, A Phys*., 304: 111903.
42. Santhoshkumar S, Murugan E. 2021. Rationally designed SERS AgNPs/GO/g-CN nanohybrids to detect methylene blue and Hg^{2+} ions in aqueous solution. *Applied Surface Science* 553: 149544.
43. Sathisha IC, K. Manjunatha, Anna Bajorek, B. Rajesh Babu, B. Chethan, T. Ranjeth Kumar Reddy, Ravikiran YT, Angadi VJ. 2020. Enhanced humidity sensing and magnetic properties of bismuth doped copper ferrites for humidity sensor applications *Jr. Alloy Compd*. 848: 156577.
44. Shah J, M. Arora, L.P. Purohit, Kotnala RK. 2011. Significant increase in humidity sensing characteristics of praseodymium doped magnesium ferrite. *Sensors Actuators, A Physics* 167: 332-337.
45. Li Y, K. Fan, H. Ban, Yang M. 2016. Detection of very low humidity using polyelectrolyte/graphene bilayer humidity sensors. *Sensors Actuators, B Chemistry* 222: 151-158.
46. Chen Z, Lu C. 2005. Humidity Sensors: A Review of Materials and Mechanisms. *Sens. Letters* 3: 274-295.
47. Sunilkumar A, S. Manjunatha, B. Chethan, Y.T. Ravikiran, T. Machappa, Masuelli M. 2019. Polypyrrole–Tantalum disulfide composite: An efficient material for fabrication of room temperature operable humidity sensor. *Sensors Actuators, A Physics* 298: 111593.
48. Zhang D, D. Wang, P. Li, X. Zhou, X. Zong, Dong G. 2018. Facile fabrication of high-performance QCM humidity sensor based on layer-by-layer self-assembled polyaniline/graphene oxide nanocomposite film. *Sensors Actuators, B Chemistry* 255: 1869-1877.
49. Ravinder D, Kumar KV. 2001. Dielectric behaviour of erbium substituted Mn-Zn ferrites. *Bull. Mater. Science* 24: 505-509.
50. Lumina Sonia MM, S. Anand, V. M. Vinosel, M. A. Janifer, S. Pauline, Manikandan A. 2018. Effect of lattice strain on structure, morphology and magneto-dielectric properties of $NiGd_xFe_{2-x}O_4$ ferrite nano-crystallites synthesized by sol-gel route. *Jr. Magn. Magn. Mater*. 466: 238-251.
51. Velanganni S, A. Manikandan, J. J. Prince, C. N. Mohan, Thiruneelakandan R. 2018. Nanostructured ZnO coated Bi_2S_3 thin films: Enhanced photocatalytic degradation of Methylene blue dye. *Physica B: Condensed Matter* 545: 383-389.
52. Baykal A, S. Guner, H. Gungunes, K.M. Batoo, Md. Amir, Manikandan A. 2018. Magneto Optical Properties and hyperfine interactions of Cr^{3+} ion substituted copper ferrite nanoparticles. *Jr. Inorg. Organomet. Polym*. 28: 2533-2544,
53. Amir M, H. Gungunes, Y. Slimani, N. Tashkandi, H.S. El Sayed, F. Aldakheel, M. Sertkol, H. Sozeri, A. Manikandan, I. Ercan, Baykal A. 2018. Mossbauer studies and magnetic properties of cubic $CuFe_2O_4$ nanoparticles. *Jr. Supercond. Nov. Magn*. 32: 557-564.
54. Slimani Y, H. Gungunes, M. Nawaz, A. Manikandan, H.S. El Sayed, M.A. Almessiere, H. Sozeri, S.E. Shirsath, I. Ercan A. 2018. Baykal, Magneto-optical and microstructural properties of spinel cubic copper ferrites with Li-Al co-substitution. *Ceram. Int*. 44: 14242-14250,
55. Lynda IJC, M. Durka, A. Dinesh, A. Manikandan, S. K. Jaganathan, A. Baykal SA. 2018. Antony, Enhanced Magneto-optical and Photocatalytic Properties of Ferromagnetic $Mg_{1-y}Ni_yFe_2O_4$ ($0.0 \leq y \leq 1.0$) Spinel Nano-ferrites. *Jr. Supercond. Nov. Magn*., 31: 3637-3647.
56. Asiri S, M. Sertkol, H. Gungunes, Md Amir, A. Manikandan, I. Ercan, Baykal A. 2018. The temperature effect on magnetic properties of $NiFe_2O_4$ nanoparticles. *Jr. Inorg. Organomet. Polym*. 28: 1587-1597,
57. Amir M, H. Gungunes, A. Baykal, M. Almessiere, H. Sozeri, I. Ercan, M. Sertkol, S. Asiri, Manikandan A. 2018. Effect of annealing temperature on Magnetic and Mossbauer properties of $ZnFe_2O_4$ nanoparticles by sol-gel approach. *Jr. Supercond. Nov. Magn*., 31: 3347-3356.
58. Abraham AG, A. Manikandan, E. Manikandan, S. Vadivel, S. K. Jaganathan, A. Baykal, Renganathan PS. 2018. Enhanced magneto-optical and photo-catalytic properties of transition metal cobalt (Co^{2+} ions) doped spinel $MgFe_2O_4$ ferrite nanocomposites. *Jr. Magn. Magn. Mater*. 452: 380-388.

59. Ratnayake SP, M Mantilaka, C Sandaruwan, D Dahanayake, Murugan E. 2019. Carbon quantum dots-decorated nano-zirconia: a highly efficient photocatalyst. *Appl. Catal. A: General* 570: 23-30.
60. Abraham AG, A. Manikandan, E. Manikandan, S. K. Jaganathan, A. Baykal, Renganathan PS. 2017. Enhanced Opto-Magneto Properties of $Ni_xMg_{1-x}Fe_2O_4$ ($0.0 \leq x \leq 1.0$) Ferrites Nano-Catalysts. *Jr. Nanoelect. Optoelect*. 12: 1326-1333.
61. Muthukrishnaraj, S. A. Al-Zahrani, A. Al Otaibi, S. S. Kalaivani, A. Manikandan, N. Balasubramanian, A. L. Bilgrami, M. A. R. Ahamed, A. Khan, A. M. Asiri, Balasubramanian N. 2021. Enhanced Photocatalytic Activity of Cu_2O Cabbage/RGO Nanocomposites under Visible Light Irradiation. *Polymers* 13: 1712.
62. Vanitha M, G. Ramachandran, A. Manikandan, Y. Slimani, M. A. Almessiere, A. Baykal, Dash CS. 2021. Effect of Sr^{2+} ions substituted nickel ferrite nanoparticles prepared by a simple microwave combustion method. *Jr. Supercond. Nov. Magn*. 34: 971-980.
63. Vinosha PA, A. Manikandan, A. S. J. Ceicilia, A. Dinesh, G. F. Nirmala, A. C. Preetha, Y. Slimani, M.A. Almessiere, A. Baykal, Xavier B. 2021. Review on recent advances of zinc substituted cobalt ferrite nanoparticles: Synthesis characterization and diverse applications. *Ceram. Int*. 47: 10512-10535.
64. Vinosha PA, A. Manikandan, R. Ragu, Y. Slimani, A. Baykal, Xavier B. 2021. Impact of nickel substitution on structure, magneto-optical, electrical and acoustical properties of cobalt ferrite nanoparticles. *Jr. Alloy Compd*. 857: 157517.
65. Vinoshac PA, A. Manikandan, A. C. Preetha, A. Dinesh, Y. Slimani, M.A. Almessiere, A. Baykal, Belina Xavier, Nirmala GF. 2021. Review on recent advances of synthesis, magnetic properties and water treatment applications of cobalt ferrite nanoparticles and nanocomposites. *Jr. Supercond. Nov. Magn*. 34: 995-1018.